

Preferential Repair of DNA Double-strand Break at the Active Gene *in Vivo*^{*[5]}

Received for publication, March 20, 2012, and in revised form, August 20, 2012. Published, JBC Papers in Press, August 21, 2012, DOI 10.1074/jbc.M112.364661

Priyasri Chaurasia[‡], Rwik Sen[‡], Tej K. Pandita[§], and Sukesh R. Bhaumik^{†1}

From the [‡]Department of Biochemistry and Molecular Biology, Southern Illinois University, School of Medicine, Carbondale, Illinois 62901 and the [§]Department of Radiation Oncology, University of Texas Southwestern Medical Center, Dallas, Texas 75390

Background: To determine whether DNA double-strand break (DSB) repair is coupled to transcription, we analyzed DSB repair at the active and inactive genes.

Results: Our results reveal that DSB repair at the active gene is faster than that at the inactive gene.

Conclusion: These results demonstrate a preferential DSB repair at the active gene.

Significance: This study supports the existence of transcription-coupled DSB repair.

Previous studies have demonstrated transcription-coupled nucleotide/base excision repair. We report here for the first time that DNA double-strand break (DSB) repair is also coupled to transcription. We generated a yeast strain by introducing a homing (Ho) endonuclease cut site followed by a nucleotide sequence for multiple Myc epitopes at the 3' end of the coding sequence of a highly active gene, *ADH1*. This yeast strain also contains the Ho cut site at the nearly silent or poorly active mating type α (*MAT α*) locus and expresses Ho endonuclease under the galactose-inducible *GALI* promoter. Using this strain, DSBs were generated at the *ADH1* and *MAT α* loci in galactose-containing growth medium that induced *HO* expression. Subsequently, yeast cells were transferred to dextrose-containing growth medium to stop *HO* expression, and the DSB repair was monitored at the *ADH1* and *MAT α* loci by PCR, using the primer pairs flanking the Ho cut sites. Our results revealed a faster DSB repair at the highly active *ADH1* than that at the nearly silent *MAT α* locus, hence implicating a transcription-coupled DSB repair at the active gene *in vivo*. Subsequently, we extended this study to another gene, *PHO5* (carrying the Ho cut site at its coding sequence), under transcriptionally active and inactive growth conditions. We found a fast DSB repair at the active *PHO5* gene in comparison to its inactive state. Collectively, our results demonstrate a preferential DSB repair at the active gene, thus supporting transcription-coupled DSB repair in living cells.

Cellular DNA is continuously attacked by both endo- and exogenous factors causing DNA damage (1–3). The most versatile cellular pathway for dealing with a large variety of structurally unrelated DNA lesions is nucleotide excision repair

(NER),² which mainly removes helix-distorting lesions, including UV-induced cyclobutane pyrimidine dimers, 6-4 photo-products, and 4-nitroquinoline-1-oxide-induced bulky chemical adducts. The other frequent damages, like oxidative lesions and small base alterations, are processed by base excision repair (4). The very toxic DNA DSBs induced by ionizing radiation are repaired via homologous recombination (HR) or non-homologous endjoining (5–8). Further, the occurrence of DNA lesions triggers checkpoints at the key stages in the cell cycle. Checkpoints monitor the progression of cell cycle post-DNA damage and maintain the proper order of events (3, 9–11). The up-regulation activity of checkpoint proteins in response to DNA damage will impose a temporary arrest of cell cycle progression to allow DNA repair or to induce apoptosis (cell death).

Although DSB is a threat to the genomic integrity of a cell, it occurs during normal DNA metabolism such as replication, meiosis, and immune system development. Programmed DSBs in meiosis are found to promote several major events beyond recombination and synaptonemal complex formation (5, 12). Cells can take advantage of DSB-induced recombination to generate genetic diversity in physiological processes such as meiosis and generation of antibodies by V(D)J recombination in lymphocytes.

An extremely cytotoxic ramification of DNA damage is when lesions in the actively transcribed coding sequence cause stalling of the transcription machinery (13, 14). Persistent transcriptional arrest interferes with cellular function or triggers apoptosis (15, 16), and thus the efficient removal of lesions from the coding regions of active genes is essential for proper cellular function. A specific repair mode, referred to as transcription-coupled repair, removes lesions from the coding sequences of active genes in both prokaryotes and eukaryotes (17–24). In prokaryotes, the transcription repair coupling factor displaces DNA damage-stalled RNA polymerase, which facilitates the recruitment of the DNA repair machinery to the lesion in the active gene. Eukaryotic transcription-coupled repair is consid-

* This work was supported, in whole or in part, by National Institutes of Health Grant 1R15GM088798-01 (to S. R. B.), American Heart Association Grant-in-Aid 10GRNT4300059 (Greater Midwest Affiliate), a Mallinckrodt Foundation grant, and Excellence in Academic Medicine (EAM) grants of the Southern Illinois University School of Medicine. This work was also supported by Grants R01 CA123232, R01 CA129537, and R01 CA154320 (to T. K. P.).

[5] This article contains supplemental Figs. S1 and S2.

¹ To whom correspondence should be addressed: sbhaumik@siumed.edu; Tel.: 618-453-6479; Fax: 618-453-6440.

² The abbreviations used are: NER, nucleotide excision repair; DSB, double-strand break; HR, homologous recombination; TC-NER, transcription-coupled NER; GG-NER, global genome NER; YPG, yeast extract, peptone plus 2% galactose; YPR, yeast extract, peptone plus 2% raffinose; YPD, yeast extract, peptone plus 2% dextrose; Pi, inorganic phosphate.

erably more complex and is not well understood, although the phenomenon of transcription-coupled repair in eukaryotes was reported more than 20 years ago (19, 21, 22).

Transcription-coupled repair is one of the two subpathways of NER. The other one is the global genome repair (GGR or GG-NER) that is responsible for the removal of DNA lesions throughout the genome. The basic steps of NER are: 1) recognition of the DNA lesion, 2) dual incisions of the DNA strand carrying the lesion to form a 24–32-nucleotide oligomer, 3) release of the excised oligomer bracketing the lesion, 4) repair synthesis to fill in the resulting gap using the undamaged strand as template, and, finally, 5) ligation. DNA damage recognition differs between GG-NER and TC-NER, but the subsequent steps are shared. The damage recognition step makes TC-NER a faster process than GG-NER. In TC-NER, recognition of the lesion is tied to RNA polymerase stalling at the DNA damage site and involves Rad26p in yeast or Cockayne syndrome group B protein (CSB) in humans (25–34). Like TC-NER, base excision repair is also coupled to transcription (35–37). However, it is yet to be determined whether DSB repair is coupled to transcription. Here, we report a fast DSB repair at the transcriptionally active gene as compared with the inactive gene, thus implying transcription-coupled DSB repair.

EXPERIMENTAL PROCEDURES

Plasmids—The plasmid pFA6a-13Myc-KanMX6 (38) was used for genomic myc epitope tagging of Ino80p at the C-terminal. The same plasmid was also used to insert the Ho cut site just before multiple myc epitope tags at the *ADH1* and *PHO5* coding sequences. The plasmid pFA6a-3HA-His3MX6 (38) was used for genomic HA epitope tagging of Rad50p and Ku70p at their C-terminals. The plasmid pRS406 (39) was used to knock out *RAD52* and *DNL4*.

Strains—The yeast (*Saccharomyces cerevisiae*) strain JKM179 contains a Ho cut site at the *MAT α* locus and expresses *HO* under the *GAL1* promoter in galactose-containing growth medium. JKM179 was obtained from the Haber laboratory (40). The genotype of JKM179 is *ho Δ MAT α hml Δ ::ADE1 hmr Δ ::ADE1 ade1–100 leu2–3,112lys5 trp1::hisG⁺ ura3–52 ade3::GAL::HO*. The Ho cut site followed by a nucleotide sequence encoding multiple myc epitope tags was added before the stop codons at the original chromosomal loci of *ADH1* and *PHO5* in JKM179 to generate the PCY23 and RSY33 strains, respectively. Multiple myc epitope tags were added to the chromosomal locus of *INO80* in JKM179 to generate the ASY32 strain. Likewise, multiple HA epitope tags were added to the chromosomal loci of *RAD50* and *KU70* in PCY23 to generate the RSY30 and RSY31 strains, respectively. The *RAD52* and *DNL4* genes were knocked out in PCY23 to generate the PCY36 and PCY37a strains, respectively.

Growth Media—For induction of the *GAL1* promoter to express *HO*, yeast cells were grown in galactose-containing medium (YPG) (yeast extract, peptone plus 2% galactose). To stop the expression of *HO*, yeast cells were grown in raffinose-containing (YPR) (yeast extract, peptone plus 2% raffinose) or dextrose-containing (YPD) (yeast extract, peptone plus 2% dextrose) medium. To study the DSB repair at the Ho cut sites at *ADH1* and *MAT α* loci, yeast cells were initially grown in YPG

and subsequently switched to YPD as described in the legend for Fig. 3B. To study DSB repair at the Ho cut site at *PHO5*, yeast cells (RSY33) were initially grown in YPG without inorganic phosphate (Pi) and then switched to YPD (transcriptionally inactive condition) or YPD-P_i (transcriptionally active condition), as described in the legend for Fig. 6, B and C.

Genomic DNA Preparation—The genomic DNA was extracted from 5 ml of yeast culture. Briefly, the harvested cells were suspended in 200 μ l of lysis buffer (50 mM HEPES (pH 7.5), 140 mM NaCl, 1 mM EDTA, 1% Triton X-100, and 0.1% Nadeoxycholate) with 200 μ l of volume-equivalent of glass beads and then vortexed for 30 min at 4 °C using a Tomy vortexer (MT-360). The whole-cell extract was collected by punching a hole at the bottom of the Eppendorf tube and then partitioned with 200 μ l of phenol:chloroform:isoamylalcohol. The aqueous phase following phenol:chloroform extraction was treated with ethanol to precipitate genomic DNA.

Analysis of DSB and Its Repair—The genomic DNA was analyzed for Ho-induced DSB and repair at the *ADH1*, *PHO5*, and *MAT α* loci using the primer pairs flanking the Ho cut sites at the *ADH1*, *PHO5*, and *MAT α* loci. The primer pair used to analyze DSB at the Ho cut site at *ADH1* was as follows: 5'-CTGGTTACACCCACGACGGTTCTT-3' and 5'-CCGAGATTTCATCAACTCATTGCTGG-3'. The primer pair used to analyze DSB at the Ho cut site at *PHO5* was 5'-ACCTCTAAT-TCTAAGAGATGTCATGAC-3' and 5'-GAATTCGAGCTC-GTTTAAAC-3'. The primer pair used to analyze the DSB at the Ho cut site at the *MAT α* locus was 5'-AGTATGCTGGA-TTTAAACTCATCTGTGATTTGTGG-3' and 5'-GATGCT-AAGAATTGATTGTTTGCCTTGAG-3'.

The disappearance of the PCR signal would indicate the presence of a DSB. A specific region of *SMC2* was amplified as a control. *SMC2* is not damaged by Ho. The primer pair for amplification of a specific region of *SMC2* was 5'-GACGACCTTGTAACAGTCCAGACAG-3' and 5'-GGCGAATTCCATCACATTATACTAACTACGG-3'.

ChIP Assay—The ChIP assay was performed as described previously (41–44). Briefly, yeast cells were treated with 1% formaldehyde, collected, and resuspended in lysis buffer. Following sonication, cell lysate (400 μ l of lysate from 50 ml of yeast culture) was precleared by centrifugation, and then 100 μ l of lysate was used for each immunoprecipitation. Immunoprecipitated protein-DNA complexes were treated with proteinase K, the cross-links were reversed, and DNA was purified. Immunoprecipitated DNA was dissolved in 20 μ l of TE 8.0 (10 mM Tris HCl (pH 8.0) and 1 mM EDTA), and 1 μ l of immunoprecipitated DNA was analyzed by PCR. PCR reactions contained [α -³²P]dATP (2.5 μ Ci for a 25- μ l reaction), and the PCR products were detected by autoradiography after separation on a 6% polyacrylamide gel. As a control, “input” DNA was isolated from 5 μ l of lysate without going through the immunoprecipitation step, and dissolved in 100 μ l of TE 8.0. To compare PCR signal arising from the immunoprecipitated DNA with the input DNA, 1 μ l of input DNA was used in the PCR analysis.

For analysis of recruitment of Ino80p, Ku70p, and Rad50p, the above ChIP protocol was modified as described previously (25). Briefly, a total of 800 μ l of lysate was prepared from 100 ml of yeast culture. Following sonication, 400 μ l of lysate was used

Preferential DSB Repair at the Active Gene

for each immunoprecipitation (using 10 μ l of anti-HA or anti-myc antibody and 100 μ l of protein A/G plus agarose beads from Santa Cruz Biotechnology, Inc.), and an immunoprecipitated DNA sample was dissolved in 10 μ l of TE 8.0, of which 1 μ l was used for the PCR analysis. In parallel, the PCR analysis for input DNA was performed using 1 μ l of DNA that was prepared by dissolving purified DNA from 5 μ l of lysate in 100 μ l of TE 8.0. The primer pairs used for PCR analysis were as follows: *MAT α* -Ho, 5'-GGTTTTGTAGAGTGGTTGACG-AAT-3' and 5'-GCTATACTGACAACATTTCAGTACTCG-3'; *ADH1*-ORF, 5'-CGGTAACAGAGCTGACACCAG-AGA-3' and 5'-ACGTATCTACCAACGATTTGACCC-3'; *ADH1*-UAS, 5'-GAGTTTCCGGGTGTACAATATGG-3' and 5'-CTATTGTATATCTCCCCTCCGC-3'; *ADH1*-Core, 5'-GGTATACGGCCTTCCTTCCAGTTAC-3' and 5'-GAACG-AGAACAATGACGAGGAAACAAAAG-3'; *PHO5*-ORF, 5'-ACCTCTAATTCTAAGAGATGTCATGAC-3' and 5'-ACA-ATGTCATCATTGGCATCGTAGTC-3'; and Chr-V, 5'-GGC-TGTCAGAATATGGGGCCGTAGTA-3' and 5'-CACCCG-AAGCTGCTTTCACAATAC-3'. UAS, upstream activating sequence; core, core promoter; and Chr-V, Chromosome-V.

Autoradiograms were scanned and quantitated by the National Institutes of Health image 1.62 program. Immunoprecipitated DNAs were quantitated as the ratio of immunoprecipitate to input in the autoradiogram.

Total RNA Preparation—Total RNA was prepared from yeast cell culture as described by Peterson *et al.* (45). Briefly, 10 ml of yeast culture was harvested and then suspended in 100 μ l of RNA preparation buffer (500 mM NaCl, 200 mM Tris-HCl, 100 mM Na₂EDTA, and 1% SDS) along with 100 μ l of phenol/chloroform/isoamyl alcohol and 100 μ l of volume-equivalent of glass beads (acid-washed, Sigma). Subsequently, the yeast cell suspension was vortexed with a maximum speed (10 in a VWR mini-vortexer, catalog no. 58816-121) five times (30 s each). The cell suspension was put in ice for 30 s between pulses. After vortexing, 150 μ l of RNA preparation buffer and 150 μ l of phenol/chloroform/isoamyl alcohol were added to the yeast cell suspension followed by vortexing for 15 s with a maximum speed on a VWR mini-vortexer. The aqueous phase was collected following 5 min of centrifugation at maximum speed in a microcentrifuge machine. The total RNA was isolated from the aqueous phase by ethanol precipitation.

RT-PCR Analysis—RT-PCR analysis was performed according to the standard protocols (46). Briefly, total RNA was prepared from 10 ml of yeast culture. Ten micrograms of total RNA was used in the reverse transcription assay. RNA was treated with RNase-free DNase (M610A, Promega) and then reverse-transcribed into cDNA using oligo(dT) as described in the protocol supplied by Promega (A3800, Promega). PCR was performed using synthesized first strand as template and the primer pairs targeted to the *ADH1* and *MAT α* ORFs. RT-PCR products were separated by 2.2% agarose gel electrophoresis and visualized by ethidium bromide staining. The primer pairs used in the PCR analysis were as follows: *ADH1*, 5'-CGGTAA-CAGAGCTGACACCAGAGA-3' and 5'-ACGTATCTACCA-ACGATTTGACCC-3' and *MAT α* , 5'-GGTTTTGTAGAGT-GGTTGACGAAT-3' and 5'-GCTATACTGACAACATT-CAGTACTCG-3'.

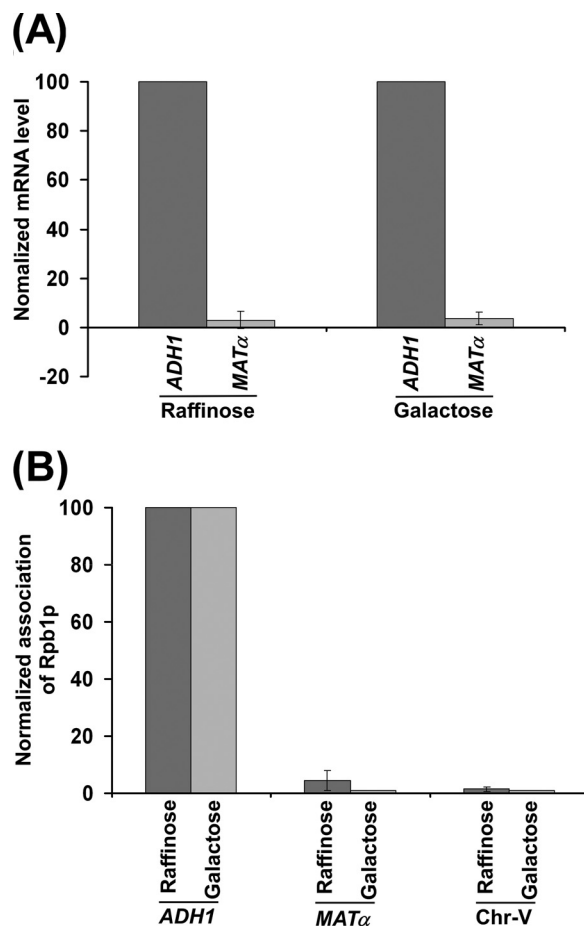


FIGURE 1. *MAT α* is a poorly active gene in comparison to a highly active *ADH1* gene. A, RT-PCR analysis of *ADH1* and *MAT α* mRNAs. Yeast cells were grown in YPR as well as YPG. Total RNA was prepared from harvested culture and analyzed for *ADH1* and *MAT α* mRNAs. The level of *ADH1* mRNA was set to 100, and *MAT α* mRNA was normalized with respect to 100. Normalized mRNA levels are plotted in the form of a histogram. B, analysis of RNA polymerase II association with the *ADH1* and *MAT α* loci. Yeast cells were grown in YPR as well as YPG and cross-linked by formaldehyde. Immunoprecipitation was performed as described previously (41–44) using a mouse monoclonal antibody 8WG16 (Covance) against the carboxyl terminal domain of the largest subunit (Rpb1p) of RNA polymerase II. Immunoprecipitated DNAs were analyzed by PCR using the primer pairs targeted to *ADH1* and *MAT α* . The ratio of the PCR signal of immunoprecipitated DNA to that of input DNA was determined and referred to as the ChIP signal. The ChIP signal at *ADH1* was set to 100, and the ChIP signals at *MAT α* and Chr-V were normalized with respect to 100. The normalized ChIP signals (represented as normalized occupancy) are plotted in the form of a histogram.

RESULTS AND DISCUSSION

Induction of DSBs at the Highly Active *ADH1* and Nearly Silent *MAT α* Genes—Cells in S-phase have a fast kinetics of DNA DSB repair post-irradiation as compared with cells in G₁ or G₂ phase (47). The fast repair kinetics of DSBs in S phase is attributed to functionally active DNA polymerases. To determine whether RNA polymerases have any influence on the repair of DNA DSB, we analyzed the effect of RNA polymerase II-dependent transcription on DSB repair by introducing the Ho cut site at the *ADH1* coding sequence and *MAT α* locus as described below. Our RT-PCR analysis revealed that *ADH1* is a highly active gene as compared with the *MAT α* locus (Fig. 1A). *MAT α* appeared to be a poorly active or nearly silent gene, consistent with previous studies (48). These observations were

further substantiated by the analysis of the association of RNA polymerase II with these two loci. We found a robust association of RNA polymerase II with *ADHI* as compared with the *MAT α* locus (Fig. 1B). A primer pair targeted to the transcriptionally inactive region of chromosome V was also used in the PCR analysis as a nonspecific DNA control (49). Collectively, these results demonstrate that *ADHI* is a highly active gene, consistent with previous studies (48, 50), and *MAT α* is a nearly silent gene as compared with *ADHI*. However, the coding sequences of both genes have a similar nucleosomal density (51).

To determine whether DSB repair is coupled to transcription, we first analyzed the DSB at the nearly silent *MAT α* locus using the yeast strain that has a Ho cut site at the *MAT α* locus and expresses *HO* under the control of the *GALI* promoter in galactose-containing growth medium (Fig. 2A). The yeast strain was initially grown in raffinose-containing medium up to an A_{600} of 0.9 and then switched to galactose-containing growth medium for 30 and 60 min. In raffinose-containing growth medium, *HO* was not expressed, as the *GALI* promoter is not induced in the presence of raffinose (44, 52). Therefore, the Ho cut site at the *MAT α* locus was intact in raffinose-containing growth medium (Fig. 2B). Upon switching to galactose-containing growth medium, *HO* was expressed as the *GALI* promoter is induced in the presence of galactose (44, 52). Such an expression of *HO* would induce a DSB at the Ho cut site at the *MAT α* locus. The generation of a DSB at the *MAT α* locus was monitored by PCR using the primer pair flanking the Ho cut site (Fig. 2A). The disappearance of the PCR signal would indicate the DSB at the *MAT α* locus. Our PCR analysis revealed that the PCR signal was significantly reduced upon switching the growth medium from raffinose to galactose for 30 and 60 min (Fig. 2B). As a control, we amplified a specific region of *SMC2* that is not damaged by Ho. We find that like the *MAT α* locus, the PCR signal at *SMC2* did not decrease upon switching the growth media from raffinose to galactose for 30 and 60 min (Fig. 2B). These results support that the expression of *HO* in galactose-containing growth medium induced DSB at the *MAT α* locus.

To further support the induction of DSB at the *MAT α* locus, we analyzed the recruitment of the INO80 complex at the Ho cut site because previous studies (53, 54) have demonstrated the recruitment of INO80 to DSB. INO80 is an ATP-dependent chromatin remodeling complex and is required to promote DSB repair (53–55). To analyze the recruitment of the INO80 complex at the *MAT α* -Ho locus, we tagged the Ino80p component of INO80 by myc epitope in the JKM179 strain that has a Ho cut site at the *MAT α* locus and expresses *HO* under the *GALI* promoter. Subsequently, the ChIP assay was performed following the switch of the growth medium from raffinose to galactose for 60 min. Immunoprecipitated chromatin was analyzed by PCR at the site proximal (represented as “ChIP region” in Fig. 2A) to the DSB. Consistent with previous studies (53, 54), we observed an enhanced recruitment of INO80 to the ChIP region in galactose-containing growth medium (Fig. 2C), thus supporting the presence of DSB at the *MAT α* locus.

Next, we analyzed the DSB at the highly active *ADHI* gene. In this direction, we introduced a Ho cut site followed by a nucle-

otide sequence for multiple myc epitope tags just before the translational stop codon of *ADHI* in the JKM179 strain. To confirm the presence of the Ho cut site at the *ADHI* locus in the generated strain (PCY23), the DSB was analyzed in raffinose, dextrose, or galactose-containing growth medium. In the raffinose- or dextrose-containing growth media, the *GALI* promoter is not induced (44, 52), and thus, *HO* would not be expressed. Hence, DSB would not be observed at the *ADHI* locus in raffinose- or dextrose-containing growth medium. The DSB at the *ADHI* locus was analyzed by PCR using the primer pair flanking the Ho cut site. The PCR signal at the *ADHI* locus disappeared in galactose-containing growth medium but not raffinose- or dextrose-containing growth medium (Fig. 2D). As a control, we amplified a specific region at the *SMC2* locus and found that the PCR signal at *SMC2* did not disappear in galactose-containing growth medium (Fig. 2D). These results demonstrate the presence of DSB (and hence the Ho cut site) at the *ADHI* locus in galactose-containing growth medium.

We next analyzed the induction of DSB at the *ADHI* locus following the switch of the growth medium from raffinose to galactose for 30 and 60 min. In this direction, we inoculated the yeast strain in raffinose-containing medium, and grown up to an A_{600} of 0.9 at 30 °C. Subsequently, yeast cells were transferred to galactose-containing growth medium for 30 and 60 min, and DSB was analyzed at the *ADHI* locus by PCR. We find a modest decrease in the PCR signals after 30 and 60 min in galactose-containing growth medium (Fig. 2E). The PCR signal at the control *SMC2* gene did not decrease after 30 and 60 min in galactose-containing growth medium (Fig. 2E). Thus, there is a modest level of DSB at *ADHI* following the switch of the growth medium from raffinose to galactose for 30 and 60 min (Fig. 2E). On the other hand, we observed a dramatic decrease in the PCR signal at the Ho cut site at the *MAT α* locus (Fig. 2B). These observations indicate that the nearly silent *MAT α* locus has significantly more DNA DSB than the highly active *ADHI* gene.

Fast DSB Repair at ADHI in Comparison to MAT α —Why is the extent of DSB at *ADHI* less than that at the *MAT α* locus? When *HO* is expressed in galactose-containing growth medium, both the generation and repair of DSB occur simultaneously, as Ho is constantly present in galactose-containing growth medium. Therefore, we do not observe 100% DSB. However, less DSB would be observed if DSB repair occurs faster than its generation in galactose-containing growth medium. Intriguingly, we observed less DSB at the highly active *ADHI* gene than the nearly silent *MAT α* locus. Thus, these observations indicate that there might be a fast DSB repair at *ADHI* as compared with the *MAT α* locus. To confirm that the DSB at the highly active *ADHI* gene is repaired fast in comparison to the nearly silent *MAT α* locus, we analyzed DSB repair at the *ADHI* and *MAT α* loci. In this direction, we grew the yeast cells in galactose-containing growth medium up to an A_{600} of 0.2 to induce maximal DSB at *ADHI* (as done in Fig. 2D) and then switched to dextrose-containing growth medium for 0.5, 2, and 3 h to allow the cells to repair the DSB as shown schematically in Fig. 3A. We isolated genomic DNAs from these yeast cultures and analyzed DSB repair by PCR using the primer pairs flanking the Ho cut sites at the *ADHI* and *MAT α* loci. The

Preferential DSB Repair at the Active Gene

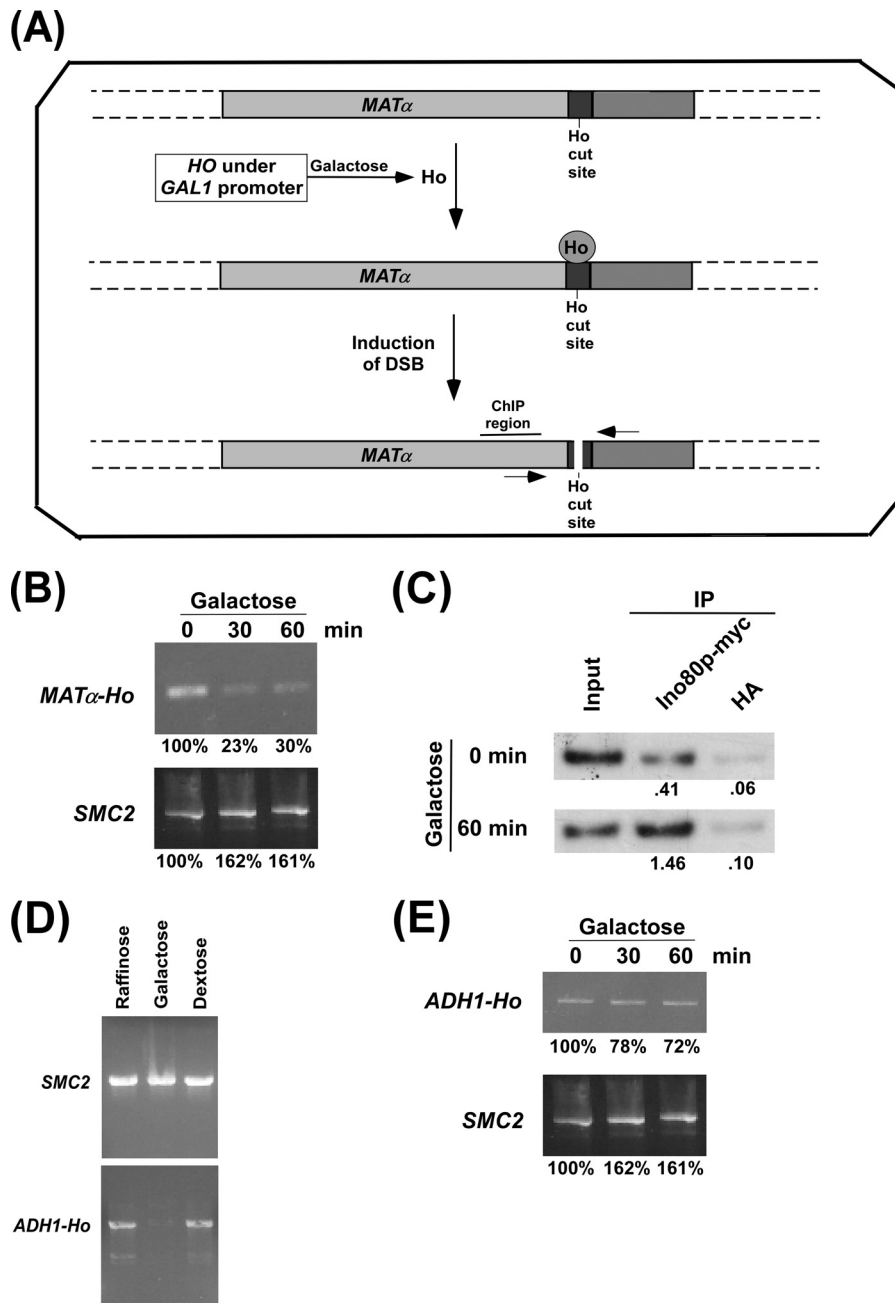


FIGURE 2. Analysis of DSB at the *MAT α* and *ADH1* loci. *A*, schematic diagram showing the generation of DSB at the *MAT α* locus following the induction of *HO* expression. The primers flanking the Ho cut site are marked by two arrow-headed lines and were used in PCR for analysis of DSB. *B*, PCR analysis of DSB at the *MAT α* locus. The yeast strain that contains a Ho cut site at the *MAT α* locus and expresses *HO* under the *GAL1* promoter was initially grown in YPR up to an A_{600} of 0.9 (log phase) and then switched to YPG for 30 and 60 min (an A_{600} of 1.0 is $\sim 3 \times 10^7$ yeast cells/ml; 46). Genomic DNA was analyzed by PCR to determine DSB using the primer pair flanking the DSB site. The PCR signal at 0 min was set to 100. The PCR signals at 30 or 60 min in YPG were normalized with respect to the 0 min time point in YPG. *C*, the CHIP assay for analyzing the recruitment of Ino80p to the DSB site. The yeast strain (ASY32) was grown as in *B* prior to cross-linking. Immunoprecipitation (IP) was performed using an anti-myc antibody (9E10, Santa Cruz Biotechnology, Inc.) against myc-tagged Ino80p. An anti-HA was used as a nonspecific antibody control. The ratio of immunoprecipitate over the input in the autoradiogram is indicated below the immunoprecipitated band. *D*, analysis of DSB at *ADH1* in YPR, YPG, and YPD media. The yeast strain PCY23 was grown in YPR, YPG, or YPD up to an A_{600} of 0.2 at 30 °C and harvested. Genomic DNA was analyzed for DSB by PCR using the primer pair flanking the HO cut site at *ADH1*. *E*, induction of DSB at the *ADH1* locus. The yeast strain PCY23 was grown as in *B*.

increase in PCR signal would indicate the progression of DSB repair. Intriguingly, we find that the PCR signal at *ADH1* increased more than that at the *MAT α* locus (Fig. 3*B*). These observations support that the DSB at the highly active *ADH1* is repaired fast as compared with the nearly silent *MAT α* locus. Therefore, we detected less DSB at *ADH1* than at the *MAT α* locus (Fig. 2, *B* and *E*).

HR-dependent DSB repair is absent at the *MAT α* locus because of the deletion of the donor in the parent JKM179 strain (40). Thus, DSB repair at the *MAT α* locus occurs via non-homologous end joining. An enhanced DSB repair at *ADH1* as compared with *MAT α* could be due to the presence of HR at *ADH1*. To test this possibility, we analyzed DSB repair at *ADH1* in the presence and absence of Rad52p that is essential

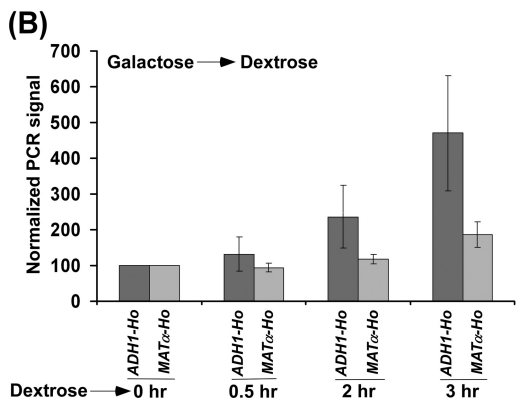
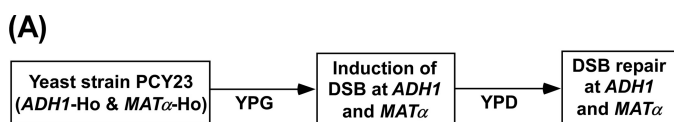


FIGURE 3. **Analysis of DSB repair at the *ADH1* and *MATα* loci.** A, schematic diagram for the experimental strategy. B, the yeast strain PCY23 was initially grown in YPG up to an A_{600} of 0.2 and then switched to YPD for 0.5, 2, and 3 h. Genomic DNAs from these yeast cultures were analyzed by PCR for DSBs at the *ADH1* and *MATα* loci. The PCR signals at the 0 h time point for both the *ADH1* and *MATα* loci were set to 100, and the signals at other time points were normalized with respect to 100. Normalized PCR signals are plotted in the form of a histogram.

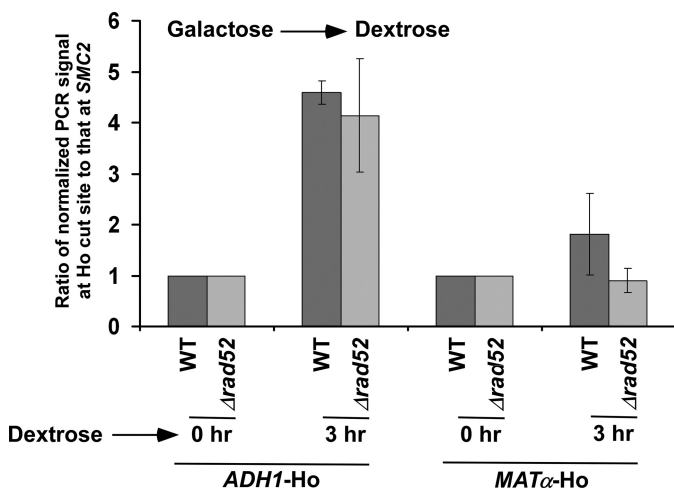


FIGURE 4. **Analysis of DSB repair at the *ADH1* and *MATα* loci in the presence and absence of *Rad52p*.** Both the wild-type (PCY23) and $\Delta rad52$ (PCY36) strains were grown as in Fig. 3B. Genomic DNAs from these yeast cultures were prepared and analyzed by PCR for DSBs at the *ADH1* and *MATα* loci. A specific region within *SMC2* was amplified as control, using the same genomic DNAs. The PCR signals at 0 h time point for the *ADH1*, *MATα* and *SMC2* loci were set to 100, and the PCR signals at 3 h were normalized with respect to 100. The ratios of normalized PCR signals at 3 h at the *ADH1* and *MATα* Ho cut sites to that at *SMC2* are plotted in the form of a histogram. A ratio that is greater than 1 would indicate the DSB repair.

for HR-dependent DSB repair (56). We find that the absence of *Rad52p* did not significantly alter the DSB repair at *ADH1* (Fig. 4). Thus, DSB repair at *ADH1* does not appear to be promoted via HR but rather non-homologous end joining. Such DSB repair is impaired in the absence of DNA ligase *Dnl4p* (Figs. 5, A and B).

How is the DSB repair facilitated at the active gene? We hypothesize that RNA polymerase II promotes the recruitment of the repair factors to the DSB site at the active gene (and hence stimulates DSB repair), analogous to the fact that RNA poly-

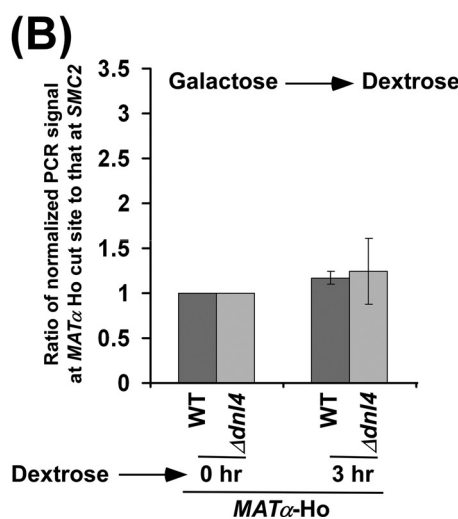
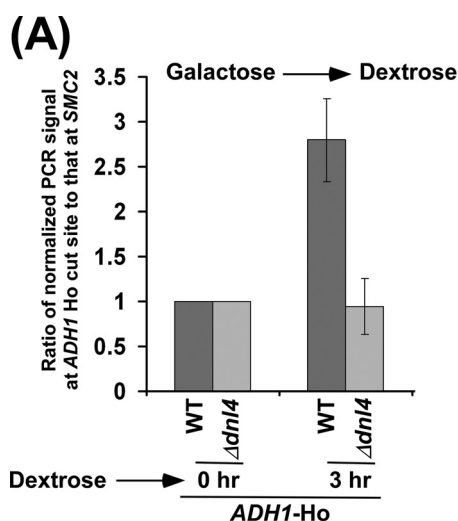


FIGURE 5. **Analysis of DSB repair at *ADH1* in the presence and absence of *Dnl4p*.** Both the wild-type (PCY23) and $\Delta dnl4$ (PCY37a) strains were grown as in Fig. 3B. The DSB repairs at the *ADH1* (A) and *MATα* (B) loci were analyzed as in Fig. 4.

merase II facilitates the recruitment of TC-NER-specific factor *Rad26p* to the DNA lesion at the active gene to promote NER (25). In support of this hypothesis, a recent study (57) implicated the interaction of RNA polymerase II with RPA (replication protein A complex), which is involved in DSB repair. Further, the INO80 chromatin remodeling complex that promotes DSB repair is recruited to the gene in a transcription-dependent manner (58, 59). Similarly, the recruitment of the MRX (*Mre11p-Rad50p-Xrs2p*) complex and *Ku* proteins to the DSB site might be promoted by RNA polymerase II or transcription machinery to stimulate DSB repair. To test this, we generated yeast strains carrying HA epitope tags at the C-terminals of *Rad50p* (*Mre11p-Rad50p-Xrs2p*) and *Ku70p* (*Ku* proteins) and then performed the ChIP experiments to analyze their association with the active *ADH1* gene. Our ChIP analysis revealed that *Rad50p* and *Ku70p* did not associate with *ADH1* (supplemental Fig. S1, A and B). Thus, RNA polymerase II or active transcription machinery does not appear to promote the targeting of *Mre11p-Rad50p-Xrs2p* or *Ku70p* to DSB. However, like the association of RPA and INO80 with the active gene (57–59),

Preferential DSB Repair at the Active Gene

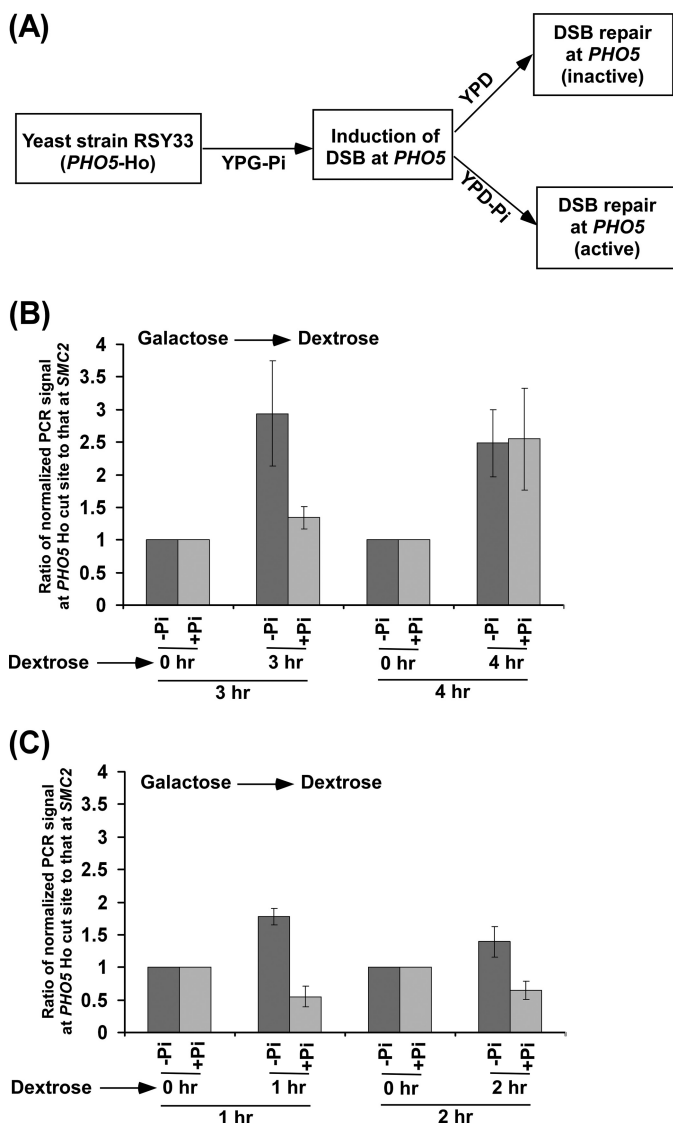


FIGURE 6. Analysis of DSB repair at the *PHO5* gene under transcriptionally inactive and active conditions. A, schematic diagram for the experimental strategy. *Inactive* and *active* refer to DSB repairs under transcriptionally inactive and active conditions, respectively. B and C, the yeast strain RSY33 was initially grown in YPG-P_i up to an A₆₀₀ of 0.4 and then switched to YPD (denoted as +Pi) or YPD-P_i (denoted as -Pi) for 1, 2, 3, and 4 h. Genomic DNAs from these yeast cultures were prepared and analyzed by PCR for DSBs at the *PHO5* locus using the primer pair flanking the Ho cut site. A specific region within *SMC2* was amplified as control using the same genomic DNAs. The PCR signals at the 0 h time point for the *PHO5* and *SMC2* loci were set to 100, and the PCR signals at 1, 2, 3, and 4 h were normalized with respect to 100. The ratios of normalized PCR signals at 1, 2, 3 and 4 h at the *PHO5* Ho cut site to those at *SMC2* are plotted in the form of a histogram. A ratio that is greater than 1 would indicate the DSB repair.

we have demonstrated recently that TC-NER factor Rad26p associates with active genes (25, 60) and facilitates chromatin disassembly (60, 61). Such chromatin regulatory function of Rad26p might be enhancing DSB repair at the active gene. Further, DSB repair at the active coding sequence is likely to be promoted by a transcription-coupled open chromatin structure or chromatin remodeling/modifying factors. These possibilities remain to be investigated. Nonetheless, this study demonstrates for the first time that DSB repair at the active gene occurs faster than that at the inactive gene, thus supporting transcription-coupled DSB repair.

Fast DSB Repair at *PHO5* under Transcriptionally Active Conditions in Comparison with the Inactive State—To extend our results to another set of transcriptionally active and inactive genes, we introduced a Ho cut site followed by a nucleotide sequence for multiple myc epitope tags just before the translational stop codon of an inducible *PHO5* gene in the aforesaid yeast (JKM179) strain that had a Ho cut site at the *MAT α* locus and expressed *HO* under the *GAL1* promoter. The *PHO5* gene is transcriptionally induced in the absence of P_i and repressed in the presence of P_i (62–65). Thus, transcription of *PHO5* would be repressed in YPD (which contains P_i) and induced in the YPD-P_i (YPD without P_i) medium. Using this generated strain, we induced DSB at the *PHO5* coding sequence in YPG-P_i (supplemental Fig. S2) and then analyzed DSB repair under transcriptionally active (YPD-P_i) and inactive (YPD) conditions, as shown schematically in Fig. 6A. We find that DSB repair at the *PHO5* coding sequence occurs fast under transcriptionally active condition as compared with the inactive state (Fig. 6, B and C). However, at the later time point (4 h), DSB repairs at the active and inactive *PHO5* were the same (Fig. 6B). Therefore, our data support a fast DSB repair at the transcriptionally active *PHO5* gene as compared with inactive *PHO5*, hence implying transcription-coupled DSB repair.

CONCLUSION

Previous studies (17–24, 35–37) have demonstrated transcription-coupled nucleotide/base excision repairs. However, it remained unknown whether transcription-coupled DSB repair exists. Here, we have developed experimental systems to analyze the induction and repair of DSBs at the active and inactive genes. Using such systems, we demonstrate that DSB repair at the active gene occurs faster than that at the inactive genomic locus. Therefore, our results support for the first time the existence of transcription-coupled DSB repair, hence providing a new regulatory process of genome repair *in vivo*.

Acknowledgments—We thank James E. Haber for the yeast strain and Geetha Durairaj, Shivani Malik, Abhijit Shukla, and Shruti Bagla for technical assistance.

REFERENCES

1. Feuerhahn, S., and Egly, J. M. (2008) Tools to study DNA repair. What's in the box? *Trends Genet.* **24**, 467–474
2. Klaunig, J. E., Kamendulis, L. M., and Hocevar, B. A. (2010) Oxidative stress and oxidative damage in carcinogenesis. *Toxicol. Pathol.* **38**, 96–109
3. Sancar, A., Lindsey-Boltz, L. A., Unsal-Kaçmaz, K., and Linn, S. (2004) Molecular mechanisms of mammalian DNA repair and the DNA damage checkpoints. *Annu. Rev. Biochem.* **73**, 39–85
4. Seeberg, E., Eide, L., and Bjoras, M. (1995) The base excision repair pathway. *Trends Biochem. Sci.* **20**, 391–397
5. Scott, S. P., and Pandita, T. K. (2006) The cellular control of DNA double-strand breaks. *J. Cell. Biochem.* **99**, 1463–1475
6. Pandita, T. K., and Richardson, C. (2009) Chromatin remodeling finds its place in the DNA double-strand break response. *Nucleic Acids Res.* **37**, 1363–1377
7. Kanaar, R., Hoeijmakers, J. H., and van Gent, D. C. (1998) Molecular mechanisms of DNA double-strand break repair. *Trends Cell Biol.* **8**, 483–489
8. Cromie, G. A., Connelly, J. C., and Leach, D. R. (2001) Recombination at

- double-strand breaks and DNA ends. Conserved mechanisms from phage to humans. *Mol. Cell* **8**, 1163–1174
9. Hartwell, L. H., and Weinert, T. A. (1989) Checkpoints. Controls that ensure the order of cell cycle events. *Science* **246**, 629–634
 10. Hartwell, L. H. (1992) Role of yeast in cancer research. *Cancer*, **69**, 2615–2621
 11. Nyberg, K. A., Michelson, R. J., Putnam, C. W., and Weinert, T. A. (2002) Toward maintaining the genome. DNA damage and replication checkpoints. *Annu. Rev. Genet.* **36**, 617–656
 12. Richardson, C., Horikoshi, N., and Pandita, T. K. (2004) The role of the DNA double-strand break response network in meiosis. *DNA Repair* **3**, 1149–1164
 13. Conaway, J. W., Shilatfard, A., Dvir, A., and Conaway, R. C. (2000) Control of elongation by RNA polymerase II. *Trends Biochem. Sci.* **25**, 375–380
 14. Sims, R. J., 3rd, Mandal, S. S., and Reinberg, D. (2004) Recent highlights of RNA-polymerase-II-mediated transcription. *Curr. Opin. Cell Biol.* **16**, 263–271
 15. Ljungman, M., and Zhang, F. (1996) Blockage of RNA polymerase as a possible trigger for UV light-induced apoptosis. *Oncogene* **13**, 823–831
 16. Yamaizumi, M., and Sugano, T. (1994) UV-induced nuclear accumulation of p53 is evoked through DNA damage of actively transcribed genes independent of the cell cycle. *Oncogene* **9**, 2775–2784
 17. Friedberg, E. C., Aguilera, A., Gellert, M., Hanawalt, P. C., Hays, J. B., Lehmann, A. R., Lindahl, T., Lowndes, N., Sarasin, A., and Wood, R. D. (2006) DNA repair. From molecular mechanism to human disease. *DNA Repair* **5**, 986–996
 18. Hanawalt, P. C., and Spivak, G. (2008) Transcription-coupled DNA repair. Two decades of progress and surprises. *Nat. Rev. Mol. Cell Biol.* **9**, 958–970
 19. Bohr, V. A., Smith, C. A., Okumoto, D. S., and Hanawalt, P. C. (1985) DNA repair in an active gene. Removal of pyrimidine dimers from the DHFR gene of CHO cells is much more efficient than in the genome overall. *Cell* **40**, 359–369
 20. Leadon, S. A. (2000) Transcription-coupled repair. A multifunctional signaling pathway. *Cold Spring Harbor Symp. Quant. Biol.* **65**, 561–566
 21. Mellon, I., Spivak, G., and Hanawalt, P. C. (1987) Selective removal of transcription-blocking DNA damage from the transcribed strand of the mammalian DHFR gene. *Cell* **51**, 241–249
 22. Smerdon, M. J., and Thoma, F. (1990) Site-specific DNA repair at the nucleosome level in a yeast minichromosome. *Cell* **61**, 675–684
 23. Sweder, K. S., and Hanawalt, P. C. (1993) Transcription-coupled DNA repair. *Science* **262**, 439–440
 24. Tornaletti, S. (2009) DNA repair in mammalian cells. Transcription-coupled DNA repair. Directing your effort where it's most needed. *Cell Mol. Life Sci.* **66**, 1010–1020
 25. Malik, S., Chaurasia, P., Lahudkar, S., Durairaj, G., Shukla, A., and Bhaumik, S. R. (2010) Rad26p, a transcription-coupled repair factor, is recruited to the site of DNA lesion in an elongating RNA polymerase II-dependent manner *in vivo*. *Nucleic Acids Res.* **38**, 1461–1477
 26. Lee, S. K., Yu, S. L., Prakash, L., and Prakash, S. (2001) Requirement for yeast RAD26, a homolog of the human CSB gene, in elongation by RNA polymerase II. *Mol. Cell Biol.* **21**, 8651–8656
 27. Lee, S. K., Yu, S. L., Prakash, L., and Prakash, S. (2002) Yeast RAD26, a homolog of the human CSB gene, functions independently of nucleotide excision repair and base excision repair in promoting transcription through damaged bases. *Mol. Cell Biol.* **22**, 4383–4389
 28. Selby, C. P., and Sancar, A. (1997) Cockayne syndrome group B protein enhances elongation by RNA polymerase II. *Proc. Natl. Acad. Sci. U.S.A.* **94**, 11205–11209
 29. Citterio, E., Van Den Boom, V., Schnitzler, G., Kanaar, R., Bonte, E., Kingston, R. E., Hoesjmakers, J. H., and Vermeulen, W. (2000) ATP-dependent chromatin remodeling by the Cockayne syndrome B DNA repair-transcription-coupling factor. *Mol. Cell Biol.* **20**, 7643–7653
 30. Bucheli, M., and Sweder, K. (2004) In UV-irradiated *Saccharomyces cerevisiae*, overexpression of Swi2/Snf2 family member Rad26 increases transcription-coupled repair and repair of the non-transcribed strand. *Mol. Microbiol.* **52**, 1653–1663
 31. Malik, S., Bagla, S., Chaurasia, P., Duan, Z., and Bhaumik, S. R. (2008) Elongating RNA polymerase II is disassembled through specific degradation of its largest but not other subunits in response to DNA damage *in vivo*. *J. Biol. Chem.* **283**, 6897–6905
 32. Christians, F. C., and Hanawalt, P. C. (1992) Inhibition of transcription and strand-specific DNA repair by α -amanitin in Chinese hamster ovary cells. *Mutat. Res.* **274**, 93–101
 33. Lee, K. B., Wang, D., Lippard, S. J., and Sharp, P. A. (2002) Transcription-coupled and DNA damage-dependent ubiquitination of RNA polymerase II *in vitro*. *Proc. Natl. Acad. Sci. U.S.A.* **99**, 4239–4244
 34. Sweder, K. S., and Hanawalt, P. C. (1992) Preferential repair of cyclobutane pyrimidine dimers in the transcribed strand of a gene in yeast chromosomes and plasmids is dependent on transcription. *Proc. Natl. Acad. Sci. U.S.A.* **89**, 10696–10700
 35. Larsen, E., Kwon, K., Coin, F., Egly, J. M., and Klungland, A. (2004) Transcription activities at 8-oxoG lesions in DNA. *DNA Repair* **3**, 1457–1468
 36. Banerjee, D., Mandal, S. M., Das, A., Hegde, M. L., Das, S., Bhakat, K. K., Boldogh, I., Sarkar, P. S., Mitra, S., and Hazra, T. K. (2011) Preferential repair of oxidized base damage in the transcribed genes of mammalian cells. *J. Biol. Chem.* **286**, 6006–6016
 37. Tsutakawa, S. E., and Cooper, P. K. (2000) Transcription-coupled repair of oxidative DNA damage in human cells. Mechanisms and consequences. *Cold Spring Harbor Symp. Quant. Biol.* **65**, 201–215
 38. Longtine, M. S., McKenzie, A., 3rd, Demarini, D. J., Shah, N. G., Wach, A., Brachat, A., Philippsen, P., and Pringle, J. R. (1998) Additional modules for versatile and economical PCR-based gene deletion and modification in *Saccharomyces cerevisiae*. *Yeast* **14**, 953–961
 39. Sikorski, R. S., and Hieter, P. (1989) A system of shuttle vectors and yeast host strains designed for efficient manipulation of DNA in *Saccharomyces cerevisiae*. *Genetics* **122**, 19–27
 40. Moore, J. K., and Haber, J. E. (1996) Cell cycle and genetic requirements of two pathways of non-homologous endjoining repair of double-strand breaks in *Saccharomyces cerevisiae*. *Mol. Cell Biol.* **16**, 2164–2173
 41. Bhaumik, S. R., and Green, M. R. (2002) Differential requirement of SAGA components for recruitment of TATA-box-binding protein to promoters *in vivo*. *Mol. Cell Biol.* **22**, 7365–7371
 42. Bhaumik, S. R., and Green, M. R. (2003) Interaction of Gal4p with components of transcription machinery *in vivo*. *Methods Enzymol.* **370**, 445–454
 43. Shukla, A., Stanojevic, N., Duan, Z., Sen, P., and Bhaumik, S. R. (2006) Ubp8p, a histone deubiquitinase whose association with SAGA is mediated by Sgf11p, differentially regulates lysine 4 methylation of histone H3 *in vivo*. *Mol. Cell Biol.* **26**, 3339–3352
 44. Bhaumik, S. R., Raha, T., Aiello, D. P., and Green, M. R. (2004) *In vivo* target of a transcriptional activator revealed by fluorescence resonance energy transfer. *Genes Dev.* **18**, 333–343
 45. Peterson, C. L., Kruger, W., and Herskowitz, I. (1991) A functional interaction between the C-terminal domain of RNA polymerase II and the negative regulator SIN1. *Cell* **64**, 1135–1143
 46. Ausubel, F. M., Brent, R., Kingston, R. E., Moore, D. D., Seidman, J. G., and Struhl, K. (2001) *Current Protocols in Molecular Biology*, Wiley, New York
 47. Pandita, T. K., and Hittelman, W. N. (1992) The contribution of DNA and chromosome repair deficiencies to the radiosensitivity of ataxia-telangiectasia. *Radiat Res.* **131**, 214–223
 48. Holstege, F. C., Jennings, E. G., Wyrick, J. J., Lee, T. I., Hengartner, C. J., Green, M. R., Golub, T. R., Lander, E. S., and Young, R. A. (1998) Dissecting the regulatory circuitry of a eukaryotic genome. *Cell* **95**, 717–728
 49. Lee, J. S., Shukla, A., Schneider, J., Swanson, S. K., Washburn, M. P., Florens, L., Bhaumik, S. R., and Shilatfard, A. (2007) Translating histone cross-talk between H2B monoubiquitination and H3 methylation by COMPASS and Dot1. *Cell* **131**, 1084–1096
 50. Li, X. Y., Bhaumik, S. R., and Green, M. R. (2000) Distinct classes of yeast promoters revealed by differential TAF recruitment. *Science* **288**, 1242–1244
 51. Jiang, C., and Pugh, B. F. (2009) A compiled and systematic reference map of nucleosome positions across the *Saccharomyces cerevisiae* genome. *Genome Biol.* **10**, R109
 52. Bhaumik, S. R., and Green, M. R. (2001) SAGA is an essential *in vivo* target

Preferential DSB Repair at the Active Gene

- of the yeast acidic activator Gal4p. *Genes Dev.* **15**, 1935–1945
53. Morrison, A. J., Highland, J., Krogan, N. J., Arbel-Eden, A., Greenblatt, J. F., Haber, J. E., and Shen, X. (2004) INO80 and γ -H2AX interaction links ATP-dependent chromatin remodeling to DNA damage repair. *Cell* **119**, 767–775
54. van Attikum, H., Fritsch, O., Hohn, B., and Gasser, S. M. (2004) Recruitment of the INO80 complex by H2A phosphorylation links ATP-dependent chromatin remodeling with DNA double-strand break repair. *Cell* **119**, 777–788
55. Tsukuda, T., Fleming, A. B., Nickoloff, J. A., and Osley, M. A. (2005) Chromatin remodelling at a DNA double-strand break site in *Saccharomyces cerevisiae*. *Nature* **438**, 379–383
56. Mortensen, U. H., Lisby, M., and Rothstein, R. (2009) *Rad52*. *Curr. Biol.* **19**, R676–677
57. Sikorski, T. W., Ficarro, S. B., Holik, J., Kim, T., Rando, O. J., Marto, J. A., and Buratowski, S. (2011) Sub1 and RPA associate with RNA polymerase II at different stages of transcription. *Mol. Cell*, **44**, 397–409
58. Conaway, R. C., and Conaway, J. W. (2009) The INO80 chromatin remodeling complex in transcription, replication and repair. *Trends Biochem. Sci.* **34**, 71–77
59. Klopf, E., Paskova, L., Solé, C., Mas, G., Petryshyn, A., Posas, F., Wintersberger, U., Ammerer, G., and Schüller, C. (2009) Cooperation between the INO80 complex and histone chaperones determines adaptation of stress gene transcription in the yeast *Saccharomyces cerevisiae*. *Mol. Cell Biol.* **29**, 4994–5007
60. Malik, S., Chaurasia, P., Lahudkar, S., Uprety, B., and Bhaumik, S. R. (2012) Rad26p regulates the occupancy of histone H2A-H2B dimer at the active genes *in vivo*. *Nucleic Acids Research* **40**, 3348–3363
61. Malik, S., and Bhaumik, S. R. (2012) Rad26p, a transcription-coupled repair factor, promotes the eviction and prevents the reassociation of histone H2A-H2B dimer during transcriptional elongation *in vivo*. *Biochemistry*, in press
62. He, Y., Swaminathan, A., and Lopes, J. M. (2012) Transcription regulation of the *Saccharomyces cerevisiae* PHO5 gene by the Ino2p and Ino4p basic helix-loop-helix proteins. *Mol. Microbiol.* **83**, 395–407
63. Barbaric, S., Luckenbach, T., Schmid, A., Blaschke, D., Hörz, W., and Korber, P. (2007) Redundancy of chromatin remodeling pathways for the induction of the yeast PHO5 promoter *in vivo*. *J. Biol. Chem.* **282**, 27610–27621
64. Adkins, M. W., Williams, S. K., Linger, J., and Tyler, J. K. (2007) Chromatin disassembly from the PHO5 promoter is essential for the recruitment of the general transcription machinery and coactivators. *Mol. Cell Biol.* **27**, 6372–6382
65. Lau, W. W., Schneider, K. R., and O'Shea, E. K. (1998) A genetic study of signaling processes for repression of PHO5 transcription in *Saccharomyces cerevisiae*. *Genetics* **150**, 1349–1359